J. Phys. B: At. Mol. Opt. Phys. **41** (2008) 115203 (7pp) doi:10.1088/0953-4075/41/11/115203

Vibrational excitation of methane by slow electrons revisited: theoretical and experimental study

R Čurík[1], P Čársky[1] and M Allan[2]

[1] J Heyrovský Institute of Physical Chemistry, Academy of Sciences of the Czech Republic, 18223 Prague 8, Czech Republic
[2] Department of Chemistry, University of Fribourg, CH-1700 Fribourg, Switzerland

E-mail: roman.curik@jh-inst.cas.cz

Received 20 February 2008, in final form 11 April 2008
Published 27 May 2008
Online at stacks.iop.org/JPhysB/41/115203

Abstract
We have calculated and measured differential and integral cross sections for vibrationally inelastic scattering of electrons by methane molecules. The calculations were carried out using the discrete momentum representation (DMR) method. We solved the two-channel Lippmann–Schwinger equation in the momentum space. The interaction between the scattered electron and the target molecule is described by the exact static-exchange potential. Correlation–polarization forces were included by a simple local density functional theory potential of Perdew and Zunger (1981 *Phys. Rev.* B **23** 5048). The cross sections calculated in this way agree very well with our measurement and with other more recent experimental data, but are larger than some older experimental and theoretical results.

1. Introduction

Knowledge of electron impact vibrational excitations of methane is important in a wide variety of technological and atmospheric applications. Methane has been identified as a source of significant infrared absorption in the atmospheres of Jupiter, Saturn, Uranus and Neptune (Broadfoot *et al* 1986). Moreover, the methane molecule is involved in the network of greenhouse gas kinetics of Earth's atmosphere. Other applications are found in gaseous discharges, gaseous laser media, radiation detectors and in electron-impact-induced chemical reactions on surfaces.

As a result of the interests from these various fields, there has been considerable amount of experimental and theoretical work devoted to the study of electron–methane collisions in the last two decades. While calculation and measurement of elastic scattering cross sections is a well-established task (for a review, see Bundschu *et al* 1997), attempts at a theoretical analysis of vibrational excitation cross sections are rather rare.

Both off-shell and adiabatic techniques were applied for a single-centre expansion method by Althorpe *et al* (1995) and for a complex Kohn variational method by Rescigno *et al* (1995). Excitations of the symmetric mode have been analysed for several T_d molecules by Cascella *et al* (2001a) using local exchange and polarization with adiabatic approximation for the motion of the nuclei. Comparison between local and separable exchange models and their impact on the adiabatic excitations of all vibrational modes for methane can be found in Cascella *et al* (2001b). The latest calculations by Nishimura and Gianturco (2002) used a more rigorous treatment of nuclear dynamics via a close-coupling formalism, although exchange and correlation–polarization effects were included in the local approximation.

In the experimental field it is important to note that several measurements of the cross sections for vibrational excitation were made and they will be listed in detail in section 4.

In this work, we therefore aim to carry out fully *ab initio* calculations for the vibrational excitations of the methane molecule with exact static-exchange contributions and a close-coupling scheme for the vibrational motion. Correlation–polarization forces are included by a density functional theory (DFT) potential introduced by Perdew and Zunger (1981). The theoretical results are evaluated by comparison with both existing experimental data and also with our new measurements, which extend the energy and angular ranges of the existing experimental cross sections.

2. Experiment

The measurements of the vibrationally inelastic cross sections were performed using a spectrometer with hemispherical energy analysers (Allan 1992, 2005b, 2007). It is equipped with a magnetic angle changer (Read and Channing 1996, Zubek 1996), which permits measurements over the entire angular range 0°–180°. The instrumental response function was determined on elastic scattering in helium and all spectra were corrected as described earlier (Allan 2005b). Absolute values of the cross sections were determined by the relative flow technique using the theoretical helium elastic cross sections of Nesbet (1979) as a reference. The confidence limit of the absolute cross section values is about ±25%. The cross sections have a narrow peak in the forward direction which is particularly difficult to measure, and whose measurement is affected by the angular resolution of the instrument, about 3°. The measurement is consequently less precise within the first ∼5°.

3. Theory

3.1. Overview of the DMR method

The vibrationally inelastic DMR method was discussed in detail by Čurík and Čársky (2003) and only a brief summary is given here. We made use of the following approximations.

- We introduce a one-electron optical potential for the interaction between the scattered electron and the charge density of the molecule. Furthermore we retain only the first term of the optical potential expansion (see, for example, Joachain 1975), ending up with the static-exchange (SE) approximation.
- The SE approximation is corrected by a model DFT potential $V_{\rm cp}$ that accounts for orbital relaxation of the bound electrons and for the correlation between the scattered electron and the bound electrons. We used the interpolation formula suggested by Perdew and Zunger (1981).
- Nuclear dynamics is described by the rotationally frozen and vibrationally harmonic approximations. Moreover, for the vibrational space of each normal mode we use only a two-state approximation. Nishimura and Gianturco (2002) have shown that the contributions from the coupling with the higher vibrational states are negligible for the CH_4 molecule in the whole energy regime from 0.5 eV to 12 eV.

These approximations allow us to describe the scattering problem via the two-channel Lippmann–Schwinger equation in the three-dimensional momentum space:

$$\langle\chi_1\boldsymbol{k}_1|\hat{T}|\chi_0\boldsymbol{k}_0\rangle = \langle\chi_1\boldsymbol{k}_1|\hat{U}|\chi_0\boldsymbol{k}_0\rangle + \sum_{i=0}^{1}\int \mathrm{d}\boldsymbol{k}\frac{\langle\chi_1\boldsymbol{k}_1|\hat{U}|\chi_i\boldsymbol{k}\rangle\langle\chi_i\boldsymbol{k}|\hat{T}|\chi_0\boldsymbol{k}_0\rangle}{k_0^2 - 2E_i - k^2 + \mathrm{i}\varepsilon}, \tag{1}$$

where $\hat{U}$ stands for twice the interaction potential $\hat{V}$, $E_0 = 0$ (for the elastic channel) is the energy of the vibrational ground state and E_1 is the energy of the first excited vibrational state. These two states are described by the vibrational functions χ_0 and χ_1, respectively. The vectors $\boldsymbol{k}_0$ and $\boldsymbol{k}_1$ represent the plane-wave functions for the incoming and outgoing electrons, respectively.

Numerical discretization (p and i run through abscissas of the radial and angular quadratures, respectively)

$$\int \mathrm{d}k \int \mathrm{d}\hat{\boldsymbol{k}}\, g(\boldsymbol{k}) \to \sum_{p}^{NRAD} w_p \sum_{i}^{NANG} w_i g(\boldsymbol{k}_{pi}) \tag{2}$$

of the integral on the rhs of equation (1) leads to a set of two-coupled matrix equations:

$$\begin{pmatrix}\mathbb{T}_{00} & \mathbb{T}_{01}\\ \mathbb{T}_{10} & \mathbb{T}_{11}\end{pmatrix} = \begin{pmatrix}\mathbb{U}_{00} & \mathbb{U}_{01}\\ \mathbb{U}_{10} & \mathbb{U}_{11}\end{pmatrix} + \begin{pmatrix}\mathbb{U}_{00} & \mathbb{U}_{01}\\ \mathbb{U}_{10} & \mathbb{U}_{11}\end{pmatrix}\cdot\begin{pmatrix}\mathbb{G}_0 & 0\\ 0 & \mathbb{G}_1\end{pmatrix} \cdot \begin{pmatrix}\mathbb{T}_{00} & \mathbb{T}_{01}\\ \mathbb{T}_{10} & \mathbb{T}_{11}\end{pmatrix}, \tag{3}$$

with the interaction matrix elements defined as follows:

$$\begin{aligned}[\mathbb{U}_{00}]_{pi,qj} &= \langle\chi_0\boldsymbol{k}_{pi}|\hat{U}|\chi_0\boldsymbol{k}_{qj}\rangle\\ [\mathbb{U}_{11}]_{pi,qj} &= \langle\chi_1\boldsymbol{k}_{pi}|\hat{U}|\chi_1\boldsymbol{k}_{qj}\rangle\\ [\mathbb{U}_{01}]_{pi,qj} &= \langle\chi_0\boldsymbol{k}_{pi}|\hat{U}|\chi_1\boldsymbol{k}_{qj}\rangle = [\mathbb{U}_{10}]_{pi,qj}.\end{aligned} \tag{4}$$

The body-fixed scattering amplitudes for the vibrational transitions are obtained by the matrix inversion in equation (3). Evaluation of the matrix elements (4) was given by Čurík and Čársky (2003). More details about the quadrature scheme (2) of the singular kernels on the rhs of equation (1) can be found in Polášek *et al* (2000) and Čársky and Čurík (2006).

3.2. Correlation–polarization potential

Several models for a potential that includes both correlation and polarization effects in electron–molecule scattering problems were proposed by Perdew and Zunger (1981), O'Connell and Lane (1983) and Padial and Norcross (1984). Since then many authors have successfully utilized a simple and local form of the correlation energy provided by these electron–gas type simulations noted above. Among these we mention applications to the elastic electron–molecule collisions (Čurík *et al* 2000) and vibrationally and rotationally inelastic processes (Cascella *et al* 2001a, Telega *et al* 2004). In contrast to most of the DFT potentials used in quantum chemistry these models do not contain exchange interaction and they are based on a hybridization of the local electron–gas theory for short distances and the asymptotic form of the polarization potential as

$$V_{\rm cp} = \begin{cases} V_{\rm c}, & r \leqslant r_0\\ V_{\rm p} = -\dfrac{\alpha_0}{2r^4}, & r > r_0\end{cases}, \tag{5}$$

where the dipole polarization potential $V_{\rm p}$ is spherically symmetric in the case of methane molecule. In the above equation r_0 is a matching radius where $V_{\rm c} = V_{\rm p}$ and α_0 is the static isotropic polarizability of the molecule. The $V_{\rm cp}$ potential (5) is energy independent and very simple to apply, depending only on the molecular charge density and polarizabilities. For its short-range part $V_{\rm c}$ we followed the

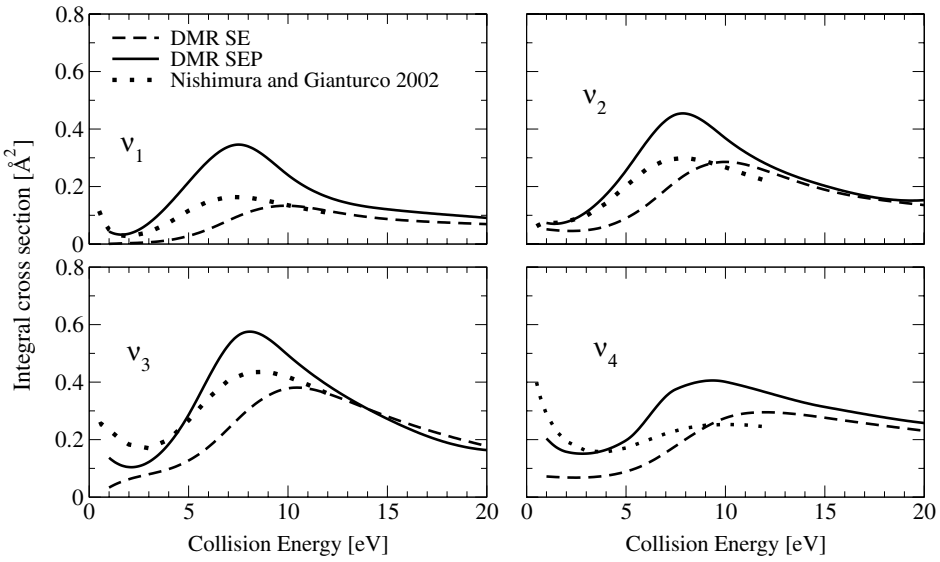

Figure 1. Rotationally summed $v = 0 \rightarrow 1$ integral cross sections for the excitation of the four vibrational modes indicated. The broken curves represent our results with the SE optical potential while the full curves also include the correlation–polarization model (SEP), summarized in equation (5). We compare our results with the calculations of Nishimura and Gianturco (2002), displayed with dotted lines.

conclusions of Padial and Norcross (1984) by choosing the form of Perdew and Zunger (1981):

$$V_c(\vec{r}) = \begin{cases} 0.0311 \ln r_s - 0.0584, \\ \quad +0.001\,33 r_s \ln r_s - 0.0084 r_s & r_s < 1 \\ \dfrac{\gamma\left(1 + \frac{7}{6}\beta_1\sqrt{r_s} + \frac{4}{3}\beta_2 r_s\right)}{(1 + \beta_1\sqrt{r_s} + \beta_2 r_s)^2}, & r_s \geqslant 1 \end{cases} \tag{6}$$

where the constants are $\gamma = -0.1423$, $\beta_1 = 1.0529$, $\beta_2 = 0.3334$ and the radius of a unity charge r_s is a function of the bound-electron density $\varrho(\vec{r})$

$$r_s = \left[\frac{3}{4\pi\varrho(\vec{r})}\right]^{1/3}. \tag{7}$$

In order to calculate the matrix elements $\mathbb{U}_{01}$ in equation (4) we also need to evaluate derivatives of V_{cp} with respect to nuclear coordinates. This leads to the necessity of knowing the derivatives of the dipole polarizabilities in equation (5) and through equations (6) and (7) to derivatives of the electron density $\varrho(\vec{r})$. Both derivatives are evaluated by the use of standard quantum chemistry software as will be described below.

3.3. Dipole polarizabilities

Isotropic dipole polarizability of CH_4 molecule has been a subject of numerous computational (Amos 1979, Wong *et al* 1991, Maroulis 1994) and experimental (Werner *et al* 1976, Hohm and Kerl 1993) studies. However the derivatives of the dipole polarizabilities are difficult to find in the literature. Therefore the first step in our computations was to determine all the independent components of polarizability tensor derivatives. We employed the linear response approach (Dalskov and Sauer 1998) in the following *ab initio* methods: second-order polarization propagator (SOPPA), multiconfiguration self-consistent field (MCSCF), coupled cluster singles and doubles (CCSD), with basis sets starting at aug-cc-pVDZ with the results being saturated at daug-cc-pVTZ (Dunning 1989, Woon and Dunning 1994) or Sadlej's basis sets (Sadlej 1988). The results for the daug-cc-pVTZ basis are summarized in table 1. Our CCSD results give polarizability derivative for the symmetric stretch R_s of the C–H bond $\partial\alpha_0/\partial R_s = 15.6$ a.u. to be compared with 15.7 a.u. calculated by Maroulis (1994). Furthermore the CCSD Born–Oppenheimer polarizability $\alpha_0 = 16.41$ a.u. needs to be corrected by an additional value of 0.88 a.u. that accounts for zero-point vibrations (Wong *et al* 1991). This correction pushes our calculated α_0 to 17.28 a.u. to be compared with the experimental value of 17.26 a.u. of Hohm and Kerl (1993). The encouraging agreement between computed polarizabilities and available experimental and theoretical data allowed us to use the CCSD values of table 1 for the following scattering calculations.

Table 1. Dipole polarizability and its non-zero derivatives calculated by several *ab initio* methods with the daug-cc-pVTZ basis set. Atomic units are used throughout the table.

Method	α_0	$\frac{\partial\alpha_{xx}}{\partial x_H}$	$\frac{\partial\alpha_{yy}}{\partial x_H}$	$\frac{\partial\alpha_{zz}}{\partial x_H}$
MCSCF	16.15	2.81	1.85	1.85
SOPPPA	16.27	2.86	1.92	1.92
CCSD	16.41	2.92	1.92	1.92

4. Results

Figure 1 shows the calculated dependence of the integral inelastic ($0 \rightarrow 1$) cross section on collision energy for all four vibrational modes. As can be seen the cross section is dominated by a broad shape resonance centred around 7.5 eV. The effect of the V_{cp} interaction defined in equation (5) appears to be negligible for the collision energies

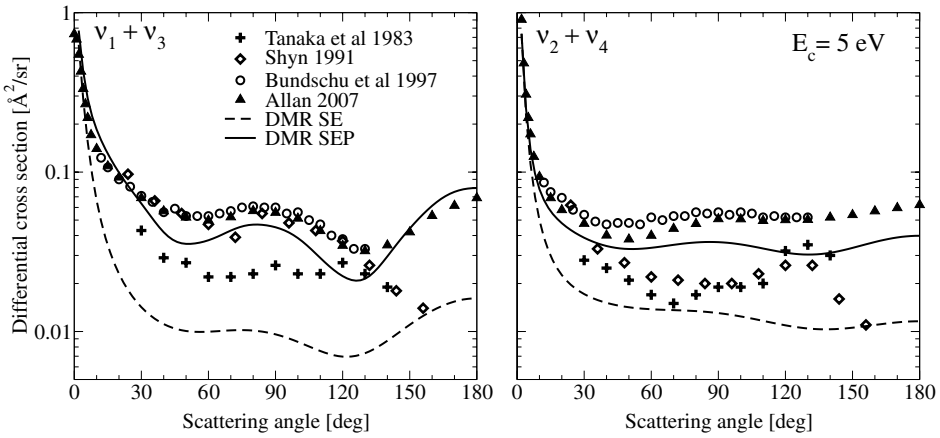

Figure 2. Rotationally summed $0 \rightarrow 1$ differential cross section for the collision energy of 5 eV. Broken curves represent our results with the SE optical potential while the solid lines also include the correlation–polarization given by equation (5) (SEP). The results of Tanaka *et al* (1983), Shyn *et al* (1991), Bundschu *et al* (1997) and Allan (2007) are shown for comparison. The left panel is for the composite stretching mode $\nu_1 + \nu_3$ and the right panel displays data for the composite deformation mode $\nu_2 + \nu_4$.

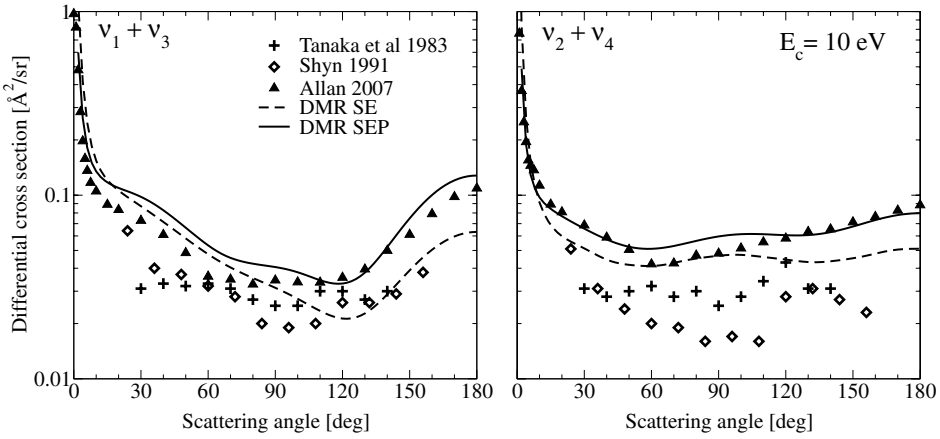

Figure 3. Rotationally summed $0 \rightarrow 1$ differential cross sections for the collision energy of 10 eV. Broken curves represent our results with the SE optical potential while the solid lines also include the SEP correlation–polarization model of equation (5). The results of Tanaka *et al* (1983), Shyn (1991) and Allan (2007) are shown for comparison. The left panel is for the composite stretching mode $\nu_1 + \nu_3$ and the right panel displays data for the composite deformation mode $\nu_2 + \nu_4$.

above 12 eV, but it shifts the shape resonance to lower energies and strongly enhances the cross section in the resonant regime. For a comparison figure 1 also displays results taken from Nishimura and Gianturco (2002). Their calculation treated nuclear dynamics in a close-coupling scheme as has been done in the present work. However, the main source of differences comes from the optical potential. The exchange part of the interaction was treated in a local semiclassical approximation in their work (Gianturco and Scialla 1987), while it is exact in the present study. Also, the previous calculations used a different correlation interaction V_c, based on the electron–electron correlation energy as suggested by Carr *et al* (1961) and Carr and Maradudin (1964). Since the magnitudes of the cross sections of Nishimura and Gianturco (2002) are somewhere between our uncorrelated and correlated results, we conclude that either their correlation interaction or their exchange interaction (or both) are weaker than those of our model.

We further evaluate the two theoretical approaches by comparing our calculated differential cross sections with available experimental data at 5 eV (in figure 2) and 10 eV (in figure 3). The present experimental data are listed for selected angles in tables 2 and 3. The two C–H stretch vibrations ν_1 and ν_3, and also the two deformation vibrations ν_2 and ν_4 cannot be entirely resolved experimentally, even with high instrumental resolution, because of the overlap of the rotational band envelopes (Müller *et al* 1985, Allan 2005a). Only the sums of the differential cross sections can meaningfully be compared with the results of calculations. Each unresolved pair contains one infrared active mode (non-zero transition dipole moment) and the angular dependence of both cross sections is therefore peaked around the forward direction, both at 5 eV and 10 eV (figures 2 and 3), as expected (Itikawa 2000). The more recent measurements, those of Bundschu *et al* (1997) and Allan (2007), are in an excellent agreement at 5 eV, while the older experiments carried out by Tanaka *et al* (1983) are

Table 2. Experimental DCS for vibrational excitation, measured as a function of scattering angle θ, at 5 eV. The units are 10^{-22} m^2 sr^{-1}.

θ	0	1	2	3	4	5	6	7.5	10
$\nu_2 + \nu_4$	251	183	90.5	48.2	30.7	21.9	17.3	12.5	9.35
$\nu_1 + \nu_3$	73.5	68.0	54.6	42.8	33.3	26.7	21.9	17.1	14.0
θ	15	20	30	40	50	60	70	80	90
$\nu_2 + \nu_4$	6.88	5.79	4.75	4.01	3.79	4.00	4.42	4.74	5.08
$\nu_1 + \nu_3$	10.9	9.27	6.89	5.69	5.20	4.98	5.22	5.71	5.57
θ	100	110	120	130	140	150	160	170	180
$\nu_2 + \nu_4$	5.07	4.95	5.01	5.03	5.20	5.39	5.69	5.96	6.23
$\nu_1 + \nu_3$	5.12	4.28	3.46	3.20	3.48	4.20	5.32	6.16	6.88

Table 3. Experimental DCS for vibrational excitation, measured as a function of scattering angle θ, at 10 eV. The units are 10^{-22} m^2 sr^{-1}.

θ	0	1	2	3	4	5	6	7.5	10
$\nu_2 + \nu_4$	234	76	37	25	19.5	15.5	14.5	13.7	11.3
$\nu_1 + \nu_3$	97	82	48	28.4	19.7	15.8	13.6	11.7	10.5
θ	15	20	30	40	50	60	70	80	90
$\nu_2 + \nu_4$	8.91	8.09	6.86	5.89	5.05	4.21	4.26	4.70	4.82
$\nu_1 + \nu_3$	8.89	8.33	7.27	6.09	4.85	3.61	3.48	3.27	3.44
θ	100	110	120	130	140	150	160	170	180
$\nu_2 + \nu_4$	5.14	5.55	5.82	6.32	6.53	7.13	7.63	8.26	8.83
$\nu_1 + \nu_3$	3.36	3.35	3.56	3.95	4.99	6.10	7.90	9.79	10.9

significantly lower. Measurements of Shyn (1991) exhibit similar behaviour for the mode $\nu_2 + \nu_4$. In the case of $\nu_1 + \nu_3$ mode the experimental data of Shyn (1991) closely follow those of Bundschu *et al* (1997) and Allan (2007); however they fall below them for scattering angles above 140°.

Note that since the experimental differential cross sections of Tanaka *et al* (1983), shown in figure 2, and of Shyn (1991) are lower than the more recent results of Bundschu *et al* (1997) and Allan (2007), they yield the integral cross sections that agree well with the calculation of Nishimura and Gianturco (2002). The present calculated cross sections, larger because of the more elaborate treatment of the exchange interactions, agree well with the more recent experimental cross sections of Bundschu *et al* (1997) and Allan (2007). For the sake of clarity not all available experimental data are included in figures 2 and 3, but a complete comparison was given by Allan (2007).

Our SEP calculations agree very well with the experiments of Bundschu *et al* (1997) and Allan (2007), both in terms of the shape and the absolute magnitude of the cross section. The agreement extends even to large scattering angles, where the data of Shyn (1991) drop, particularly at 5 eV. Figure 2 also displays the role of correlation–polarization forces in the resonant region. Although their impact is dramatic our calculated results still lie somewhat lower for the $\nu_2 + \nu_4$ mode for large scattering angles. This seems to indicate some portion of short-range part of the correlation potential V_c is missing since the quality of the short-range interaction strongly affects larger scattering angles.

The remarkable improvement brought by the inclusion of correlation and polarization is displayed even more visibly in figure 4. It shows the dependence of the differential cross section (DCS) on the collision energy for the fixed scattering angle $\vartheta = 90°$. This scattering angle was chosen because the resonance has a strong d-wave contribution resulting in a significant enhancement of the DCS for 90° (visible in the left panel of figure 2). The present experimental data are listed for selected energies in table 4.

The excellent agreement of the present SEP calculation with the present experiment and the experiment of Bundschu *et al* (1997) confirms that the present method of including correlation and polarization is successful. It works well over the entire resonant region and down to about 1 eV. The dramatic effect played by correlation and polarization at energies below about 12 eV is evident, particularly for the symmetric stretch vibration ν_1. As already stated above, the data of Tanaka *et al* (1983) and Shyn (1991) appear to be too low.

Finally, in order to complete our comparisons we also simulated electron energy-loss spectra (EELS). The sharp spectra represented by narrow vertical bars in figure 5 were spread with an energy width determined from the elastic peak of the measured spectra. This pragmatic approach bypasses the complications brought by the complex details of the rotational band envelopes (Müller *et al* 1985). As the last step we normalized the experimental spectra on the calculated elastic peak. The individual vibrations ν_2, ν_4 and ν_1, ν_3 are partially resolved in the energy-loss spectra and this form of comparison has thus the advantage of qualitatively indicating the degree of agreement for all four individual vibrations, particularly for the ν_2 and ν_4 pair. Again, figure 5 reveals an excellent agreement between the calculated and the measured cross sections for collision energies of 5 eV and 20 eV. The calculation correctly reproduces the observation that ν_2 is excited more strongly than ν_4 at 5 eV and vice versa at 20 eV.

5. Summary and conclusions

In the present calculations we used the discrete momentum representation to study the inelastic scattering of electrons

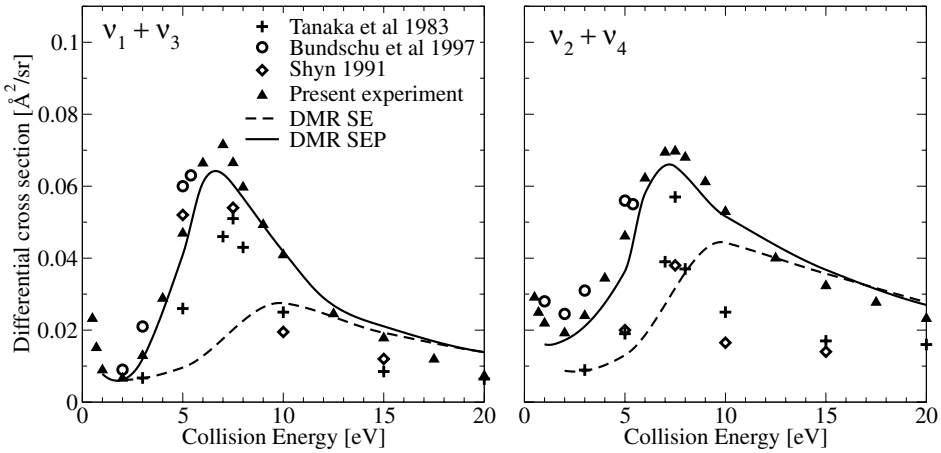

Figure 4. Rotationally summed $0 \rightarrow 1$ differential cross section as a function of the collision energy. The scattering angle is fixed at $\vartheta = 90^\circ$. Our SE and SEP results are compared with the present experimental data and the previously measured cross sections of Tanaka *et al* (1983) and Bundschu *et al* (1997). The left panel is for the composite stretching mode $\nu_1 + \nu_3$ and the right panel displays data for the composite deformation mode $\nu_2 + \nu_4$.

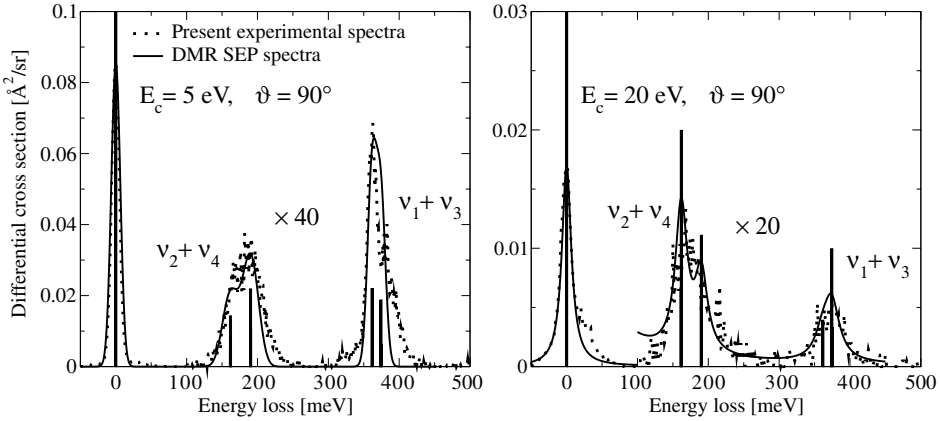

Figure 5. Computed and measured electron energy-loss spectra for the scattering angle $\vartheta = 90^\circ$. The left panel is for the collision energy $E_c = 5$ eV and the right panel is for $E_c = 10$ eV. Vertical bars represent the actual value of the differential cross section for the particular mode.

Table 4. Experimental DCS for vibrational excitation, measured as a function of the incident electron energy E, at 90°. The units are 10^{-22} m^2 sr^{-1}.

E (eV)	0.3	0.5	0.7	1.0	2.0	3.0	4.0	5.0	6.0
$\nu_2 + \nu_4$	3.42	2.91	2.49	2.19	1.92	2.40	3.44	4.62	6.22
$\nu_1 + \nu_3$	–	2.32	1.51	0.89	0.66	1.29	2.88	4.69	6.64
E (eV)	7.0	7.5	8.0	9.0	10.0	12.5	15.0	17.5	20.0
$\nu_2 + \nu_4$	6.94	6.97	6.80	6.12	5.29	4.00	3.23	2.77	2.32
$\nu_1 + \nu_3$	7.15	6.65	5.97	4.93	4.09	2.45	1.78	1.19	7.55

by the methane molecule. Our previously used (Čurík and Čársky 2003) exact static-exchange potential was extended by the local DFT-based correlation–polarization contribution originally introduced by Perdew and Zunger (1981). Our calculation correctly reproduced the existence of the broad d-wave shape resonance which dominates the vibrationally inelastic collisions around 7.5 eV and which was already known from the measurements of Tanaka *et al* (1983) and Shyn (1991) and which was found in the calculations by Nishimura and Gianturco (2002). Our present calculations predict that this resonance should be substantially more effective in enhancing vibrational excitation, however. We obtain larger cross sections for all vibrational modes, for the ν_1 and ν_4 modes by about a factor of 2, in comparison with previous calculations. These larger values are in a very good accord with the experimental findings of Bundschu *et al* (1997), Allan (2007) and with the present experiment.

The current study represents our first attempt to improve the static-exchange inelastic matrix elements (4) by a local DFT correction derived from the derivatives of equations (5)

and (6). From the good qualitative and quantitative agreements with the present experimental data and the measurements of Bundschu *et al* (1997) we conclude that such an optical potential may be successfully applied for vibrationally inelastic collisions with larger polyatomic molecules.

Acknowledgments

This work was supported by the Czech Ministry of Education (Kontakt ME857), the NSF (CHE-0446688), the project EIPAM sponsored by the European Science Foundation (grant no. PESC7-20), the Academy of Sciences of the Czech Republic (grant nos. A100400501, 1ET400400413 and KJB400400803), the Grant Agency of the Czech Republic (grant 202/08/0631) and the Swiss National Science Foundation (project no. 200020-113599/1). The calculations of polarizabilities were performed by Dr Ivana Paidarová (Heyrovský Institute, Prague) and Stephan Sauer (University of Copenhagen, Denmark). Their help is gratefully acknowledged.

References

Allan M 1992 *J. Phys. B: At. Mol. Opt. Phys.* **25** 1559
Allan M 2005a *J. Phys. B: At. Mol. Opt. Phys.* **38** 1679
Allan M 2005b *J. Phys. B: At. Mol. Opt. Phys.* **38** 3655
Allan M 2007 *Atomic and Molecular Data and Their Applications (AIP Conference Proceedings* vol 91*)* ed E Roueff (New York: American Institute of Physics) p 107
Althorpe S C, Gianturco F A and Sanna N 1995 *J. Phys. B: At. Mol. Opt. Phys.* **28** 4165
Amos R D 1979 *Mol. Phys.* **38** 33
Broadfoot A L *et al* 1986 *Science* **233** 74
Bundschu C T, Gibson J C, Gulley R J, Brunger M J, Buckman S J, Sanna N and Gianturco F A 1997 *J. Phys. B: At. Mol. Opt. Phys.* **30** 2239
Čársky P and Čurík R 2006 *Computational Chemistry: Reviews of Current Trends* vol 10 ed J Leszczynski (Singapore: World Scientific)
Carr W J, Jr, Coldwell-Horsfall R A and Fein A E 1961 *Phys. Rev.* **124** 747
Carr W J, Jr and Maradudin A A 1964 *Phys. Rev.* A **133** 371
Cascella M, Čurík R, Gianturco F A and Sanna N 2001a *J. Chem. Phys.* **114** 1989–2000
Cascella M, Čurík R and Gianturco F A 2001b *J. Phys. B: At. Mol. Opt. Phys.* **34** 705
Čurík R, Gianturco F A and Sanna N 2000 *J. Phys. B: At. Mol. Opt. Phys.* **33** 615
Čurík R and Čársky P 2003 *J. Phys. B: At. Mol. Opt. Phys.* **36** 2165
Dalskov E K and Sauer S P A 1998 *J. Phys. Chem. A* **102** 5269
Dunning T H, Jr 1989 *J. Chem. Phys* **90** 1007
Gianturco F A and Scialla S 1987 *J. Phys. B: At. Mol. Opt. Phys.* **20** 3171
Hohm U and Kerl K 1993 *Mol. Phys.* **80** 625
Itikawa Y 2000 *Phys. Essays* **13** 344
Joachain C J 1983 *Quantum Collision Theory* (Amsterdam: Elsevier) pp 577–621
Maroulis G 1994 *Chem. Phys. Lett.* **226** 420
Müller R, Jung K, Kochem K-H, Sohn W and Ehrhardt H 1985 *J. Phys. B: At. Mol. Phys.* **18** 3971
Nesbet R K 1979 *Phys. Rev.* A **20** 58
Nishimura T and Gianturco F A 2002 *J. Phys. B: At. Mol. Opt. Phys.* **35** 2873
O'Connell J and Lane N F 1983 *Phys. Rev.* A **27** 1893
Padial N T and Norcross D W 1984 *Phys. Rev.* A **29** 1742
Perdew J P and Zunger A 1981 *Phys. Rev.* B **23** 5048
Polášek M, Juřek M, Ingr M, Čársky P and Horáček J 2000 *Phys. Rev.* A **61** 032701
Read F H and Channing J M 1996 *Rev. Sci. Instrum.* **67** 2373
Rescigno T N, McCurdy C W, Orel A E and Lengsfield B H 1995 *Computational Methods for Electron–Molecule Collisions* ed W M Huo and F A Gianturco (New York: Plenum) pp 1–44
Sadlej A J 1988 *Collect. Czech. Chem. Commun.* **53** 1995
Shyn T W 1991 *J. Phys. B: At. Mol. Opt. Phys.* **24** 5169
Telega S, Bodo E and Gianturco F A 2004 *Eur. Phys. J.* D **29** 357
Tanaka H, Kubo M, Onodera N and Suziki A 1983 *J. Phys. B: At. Mol. Opt. Phys.* **16** 2861
Werner H J and Meyer W 1976 *Mol. Phys.* **31** 855
Wong A T, Bacskay G B, Hush N S and Bogaard M P 1991 *Mol. Phys.* **74** 1037
Woon D E and Dunning T H 1994 *J. Chem. Phys.* **100** 2975
Zubek M, Gulley N, King G C and Read F H 1996 *J. Phys. B: At. Mol. Opt. Phys.* **29** L239